$D\bar{D}$ correlations in fusion and cluster models

S. Banerjee and S. N. Ganguli
Tata Institute of Fundamental Research, Homi Bhabha Road, Bombay 400005, India
(Received 18 June 1985; revised manuscript received 24 October 1985)

In the framework of fusion and cluster models we have studied correlation of $D\bar{D}$ production in hadronic collisions. The major differences in these two models are found to be in the rapidity-gap and $M_{D\bar{D}}$ distributions. Both these distributions are found to be much narrower in the cluster model than in the fusion model. Comparing these two models with the available data on $D\bar{D}$ correlation at $\sqrt{s}=27$ GeV, we find that the predictions of the fusion model are in better agreement with the data than those of the cluster model.

I. INTRODUCTION

There are a number of experiments that have been performed during recent years to determine charm-production cross sections in hadronic interactions.[1-12] From these experiments the following conclusions regarding $D\bar{D}$ production may be drawn:[13-16] $\sigma\sim 20$ μb at the CERN SPS and Fermilab energies and $\sigma\gtrsim 200$ μb at the CERN ISR energies. But there is very little experimental data on the correlation of charm particles: the NA16 experiment of the LEBC-EHS collaboration have provided 9 pairs of $D\bar{D}$;[9-11] new data on $\pi^- p$ interactions at 360 GeV/c from the NA27 experiment of the same collaboration have started becoming available[17-19] and they have 53 events of well-reconstructed $D\bar{D}$ pairs. Correlation studies are expected to provide more insight into the production mechanism of charm particles.

In this paper we present a detailed comparison of two central-type production mechanisms for charm particles in hadronic collisions: (i) the standard perturbative mechanism of the fusion process (or flavor creation)[20-24] via $g+g\to c+\bar{c}$ and $q+\bar{q}\to c+\bar{c}$, where g, q, and c stand for gluon, light quark, and charm quark, and (ii) nonperturbative model[25,26] where quark-quark scattering leads to a production of cluster of mass ≈ 5 GeV which subsequently decays to $D\bar{D}+\pi$'s. It may be mentioned that both these models have been studied in detail for the production cross section, x (Feynman x) and $p_T{}^2$ (p_T is transverse momentum) distributions of charm particles in hadronic collisions. Both these models provide similar x and $p_T{}^2$ distributions for the charm in reasonable agreement with the data (see Sec. III). The following can be said regarding the production cross section. (a) In the fusion model the cross section (σ) depends strongly on the choice[27] of m_c, the mass of the charm quark, and Λ, the QCD scale parameter. The cross section increases with the decrease of m_c and the increase of Λ, e.g., the value of σ at $\sqrt{s}=27$ GeV increases from ≈ 5 to 15 μb for the variation in m_c value from 1.5 to 1.2 GeV (for a fixed value of $\Lambda=0.2$ GeV); by increasing the value of Λ from 0.2 to 0.5 GeV the value of σ increases by a factor of 2.5. (b) In the cluster model the cross section depends strongly on the choice[26] of $t_{\min}$ the minimum four-momentum transfer needed to produce the cluster, e.g., the value of σ at $\sqrt{s}=27$ GeV increases from ≈ 8 to 22 μb for the variation in $t_{\min}$ from -0.25 to -0.10 GeV^2. It is therefore clear that both these models can reproduce the production cross section of charm at SPS energies; but the predicted rise in cross section from SPS to ISR energies by both the models is only by a factor of 4—5 and not by a factor of ~ 10 as expected from ISR measurements. It may be remarked that all the measurements made at ISR are for a limited phase space, and hence large correction factors are used to deduce total cross sections.

The present work deals with the correlation between charm particles to see if the above two models can be distinguished using the available correlation data. There have been some correlation studies using the fusion mechanism[27-29] by treating the charm quark as the charm hadron. Here we have incorporated the fragmentation function of the charm quark as well as the parton transverse momentum. The paper is organized as follows. The details of the calculation in terms of fusion and cluster models are presented in Sec. II. Numerical results are presented in Sec. III and the summary in Sec. IV.

II. DETAILS OF THE CALCULATION

In this section we give the expressions for double inclusive distribution for the charm hadrons in the fusion and the cluster models.

A. Fusion model

Here the charm quarks are produced via the subprocess $a+b\to 1+2$, where a and b are the colliding partons ($gg/q\bar{q}$). The outgoing charm quarks 1 and 2 undergo fragmentation, $1\to 3$ and $2\to 4$ and lead to charm hadrons 3 and 4 (D and $\bar{D}$). The double inclusive cross section for the charm hadrons is given by the expression (for derivation see Appendix A)

$$E_3E_4\frac{d\sigma}{d^3p_3d^3p_4}=\int\frac{\hat{s}}{2\pi}\frac{d\hat{\sigma}}{d\hat{t}}\frac{E_3E_4}{E_1E_2}\frac{D(z_3)}{z_3{}^3}\frac{D(z_4)}{z_4{}^3}G_{a/A}(x_a,\mathbf{k}_{Ta},Q^2)\times G_{b/B}(x_b,\mathbf{k}_{Tb},Q^2)J\,dz_3dz_4d^2\mathbf{k}_{Tb}\ , \quad (1)$$

where $J=(4/s)\cosh y_a \cosh y_b/\sinh(y_a-y_b)$; $y_{a,b}$ are the rapidities; and s and $\hat{s}$ are the c.m. energy squared of the initial hadrons (A,B) and the colliding partons (a,b), respectively; $\hat{s}>4m_c^2$ where m_c is mass of the charm quark. $\hat{\sigma}$ is the cross section for the subprocess and $\hat{t}$ is the square of the four-momentum transfer between partons a and 1. The expression for $d\hat{\sigma}/d\hat{t}$ is taken from Combridge.[20] The fragmentation variable z for the formation of the charm hadron from the charm quark is defined by

$$z_3=|\mathbf{p}_3|/|\mathbf{p}_1|\ ,\quad z_4=|\mathbf{p}_4|/|\mathbf{p}_2|\ , \tag{2}$$

i.e., the momentum of the produced D meson is taken to be collinear to the c-quark momentum (for simplicity we have neglected the transverse momentum of the charm hadron with respect to the direction of the charm quark). (The fragmentation variable z is defined in two ways in the literature: $z=\mathbf{p}_3\cdot\mathbf{p}_1/|p_1|^2$ or E_3/E_1. In this paper we have followed the former definition. We have checked that the results do not change significantly by taking the second definition of z.) For the fragmentation function $D(z)$ we have used the following two forms:

$$\text{(a) } D(z)=\delta(1-z) \tag{3}$$

i.e., the momentum of the D meson is the same as that of the c quark; and (b) the functional form[30] which describes the experimental data of D production in e^+e^- experiments,

$$D(z)=\frac{A}{z[1-(1/z)-0.15/(1-z)]^2} \tag{4}$$

with A as the normalization constant. The function $G_{i/H}(x_i,\mathbf{k}_{Ti},Q^2)$ with $i=a,b$ describes the probability of finding the colliding parton i with the fractional longitudinal momentum as x_i and the transverse momentum as $\mathbf{k}_{Ti}$ inside the hadron H; Q^2 is taken to be $\hat{s}$ and $\hat{s}/2$ for the subprocess $q\bar{q}$ and gg, respectively. We use the following factorization ansatz[31] for G_i:

$$G_{i/H}(x_i,\mathbf{k}_{Ti},Q^2)=\frac{1}{\tilde{x}_i}F_{i/H}(x_i,Q^2)f_i(k_{Ti}) \tag{5}$$

with $\tilde{x}_i^2=x_i^2+4k_{Ti}^2/s$; $F_{i/H}(x_i,Q^2)$ is the usual structure function and $f_i(k_{Ti})$ is the transverse-momentum distribution of the colliding parton i with the condition $\int d^2\mathbf{k}_{Ti}f_i(k_{Ti})=1$.

B. Cluster model

In this model[26] a hadronic cluster is produced via quark-quark scattering. Although the clusters are mostly pionic, they have assumed a small probability ($\sim 1\%$) of producing a heavy cluster containing a charm pair ($D\bar{D}$). The cluster is assumed to have a fixed mass of 5 GeV following the arguments of Suzuki[32] that the Q value of the cluster should not be larger than 1 GeV (cluster mass $=2M_D+Q\simeq 5$ GeV) so that only pions could be there along with the heavy hadrons ($D\bar{D}$ in the present case) in thermal equilibrium. The cluster formation and decay can be illustrated as

$$q_A(\text{projectile})+q_B(\text{target})\rightarrow \text{cluster}+q_B\ ,\quad \text{cluster}\rightarrow D\bar{D}+\pi\text{'s} \tag{6}$$

where q_A,q_B are valence quarks in hadrons A and B, respectively. The fragmentation function of the cluster is assumed to be of Boltzmann type in the rest frame of the cluster,

$$E_D^*\frac{dn}{d^3p_D^*}(\text{cluster}\rightarrow D)=A\exp(-kE_D^*) \tag{7a}$$

$$=A\exp(-kP_CP_D/M)\ , \tag{7b}$$

where A is a normalization constant such that overall probability of the cluster going to D is 1%, i.e., $n=0.01$. k is the temperature parameter assumed to be 5 GeV^{-1}. It may be mentioned that the Q value of 1 GeV and k of 5 GeV^{-1} have been used successfully to describe both pion $(u,d\rightarrow\pi)$ and single charm $(c\rightarrow D)$ fragmentation functions.[32] E_D^* and p_D^* are the energy and momentum of the charm D in the rest frame of the cluster of mass M. The expression (7b) represents the fragmentation function in the invariant form with P_C and P_D as the four-momentum vectors of the cluster and the D, respectively.

Representing the cluster production and decay by $a+b\rightarrow 1+2$, and $1\rightarrow 3+4+x$, where a and b are the colliding quarks (u or d) from the incident hadrons A and B, respectively, 1 is the cluster and the final products 3 and 4 are the charm hadrons (D and $\bar{D}$), the double inclusive cross section for the production of charm hadrons 3 and 4 is given by the expression (see Appendix B for the derivation)

$$E_3E_4\frac{d\sigma}{d^3p_3d^3p_4}=\int\frac{\hat{s}}{\pi}\frac{1}{Z}D_C(1\rightarrow 3+4+x)\frac{d\hat{\sigma}}{d\hat{t}}\times\frac{F_{a/A}(x_a,Q^2)F_{b/B}(x_b,Q^2)}{x_ax_b}dx_adx_bd^2\mathbf{p}_{T1}\ , \tag{8}$$

where Z is defined in Appendix B. This expression assumes the collinear dynamics, i.e., no transverse momentum for the colliding partons; the effect of the transverse momentum in this model is not significant and hence neglected. The quantities $\hat{s}$, $x_{a,b}$, $\hat{t}$ and $F_{i/H}(x_i,Q^2)$ are described in Sec. II A; Q^2 is taken to be M^2. We have assumed independent emission of $D\bar{D}$ from the cluster fragmentation and the function $D_C(1\rightarrow 3+4+x)$ is therefore taken to be

$$D_C(1\rightarrow 3+4+x)=C\exp[-k(P_3P_1+P_4P_1)/M] \tag{9}$$

with $M_x^2\geq 0$ and P_i's are the four-momentum vectors as defined in (B1); C is a normalization constant. The expression for $d\hat{\sigma}/d\hat{t}$ is taken to be[26]

$$\frac{d\hat{\sigma}}{d\hat{t}}=\frac{4}{9}\frac{\pi\alpha^2(Q^2)}{\hat{s}^2}\frac{\hat{u}^2+\hat{s}^2}{\hat{t}^2} \tag{10}$$

with $\hat{s}+\hat{t}+\hat{u}=M^2$ and $\alpha(Q^2)$ as the QCD running coupling constant and a lower limit of $|\hat{t}|$ as 0.25 GeV^2 (Ref. 26).

III. NUMERICAL RESULTS

The numerical calculations are carried out by using the following parametrizations for the structure functions of the proton and the pion. (a) Proton: valence quarks as given by Buras and Gaemers,[33] sea quarks as given by Owens and Reya[34] with the counting rule corrected by the QCD Q^2 evolution and gluon distribution from the neutrino data of the CDHS collaboration.[35] (b) Pion: valence, sea, and gluons as given by Owens and Reya[34]

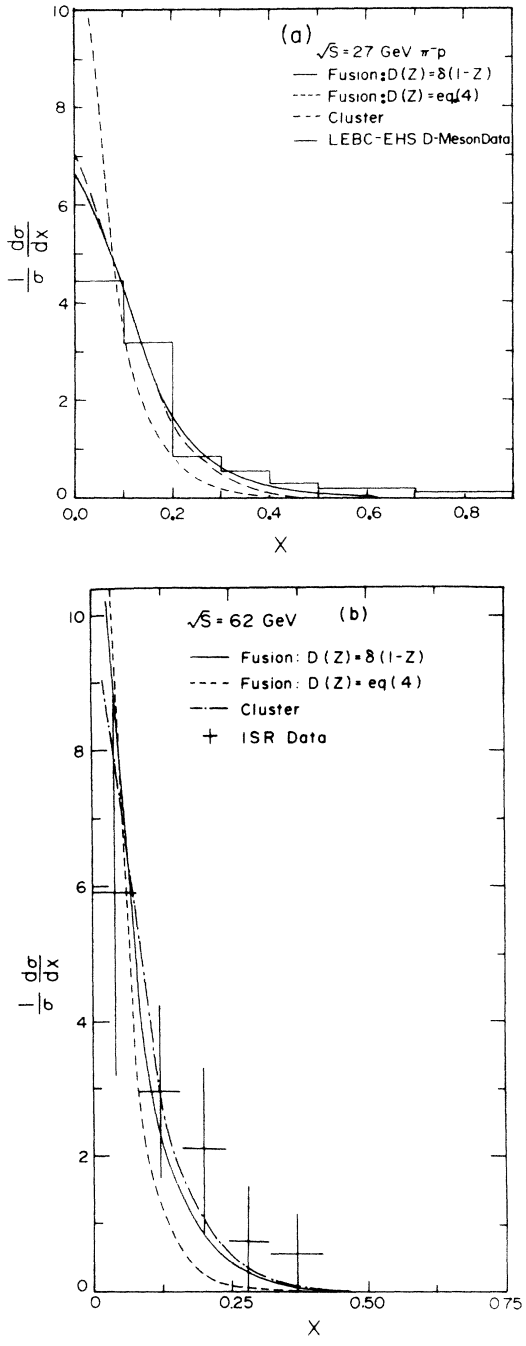

FIG. 1. Normalized differential distribution $(1/\sigma)d\sigma/dx$ as a function of Feynman x for inclusive charm-meson production in (a) $\sqrt{s}=27$ GeV $\pi^- p$ (b) $\sqrt{s}=62$ GeV pp interactions. The solid and dashed curves are results of fusion-model calculations with $\langle k_T \rangle = 0.5$ GeV/c and two forms of fragmentation functions, viz., $D(z)=\delta(1-z)$ and $D(z)=$Eq. (4), respectively. The dash-dotted curves are predictions of the cluster model with cluster mass of 5 GeV. Experimental data refer to (a) LEBC-EHS experiment (Ref. 18) and (b) ISR experiment (Refs. 7 and 8).

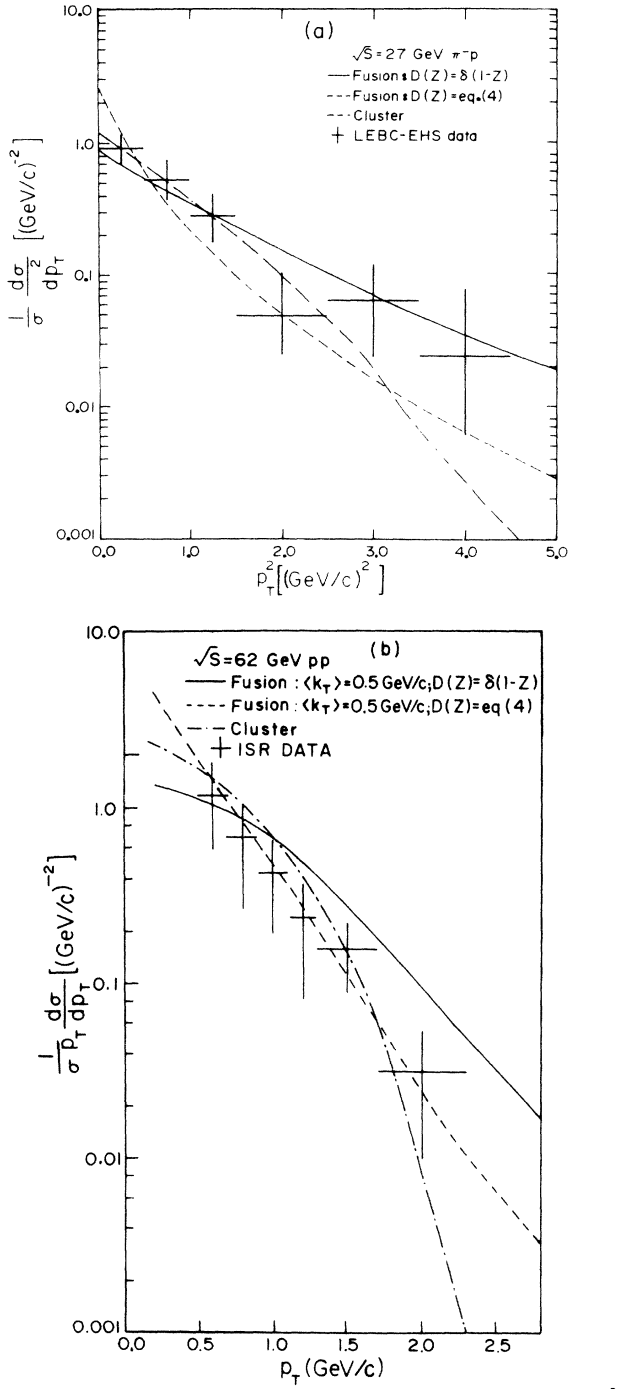

FIG. 2. (a) Normalized inclusive distribution $(1/\sigma)d\sigma/dp_T{}^2$ as a function of transverse momentum squared $p_T{}^2$ of D's at $\sqrt{s}=27$ GeV. (b) Normalized distribution $(1/\sigma)(1/p_T)d\sigma/dp_T$ as a function of p_T of D's at $\sqrt{s}=62$ GeV. The nomenclatures of the smooth curves are as in Fig. 1. Experimental data refer to (a) LEBC-EHS experiment (Ref. 18) and (b) ISR experiment (Refs. 7 and 8).

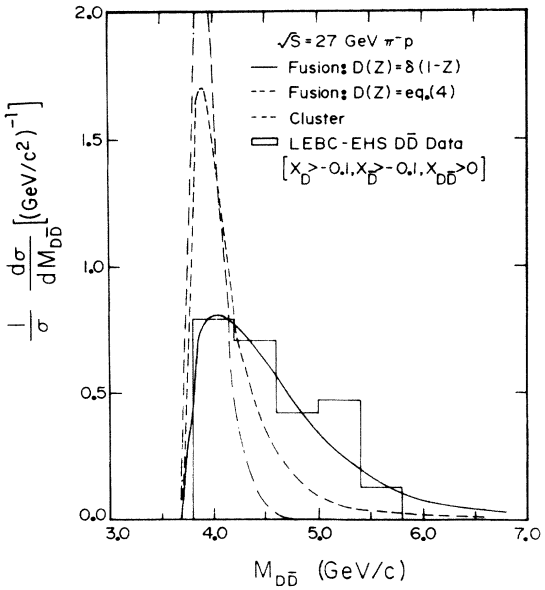

FIG. 3. Normalized distribution $(1/\sigma)d\sigma/dM_{D\bar{D}}$ as a function of $D\bar{D}$ effective mass $M_{D\bar{D}}$. The histogram refers to the LEBC-EHS experiment (Ref. 19) at $\sqrt{s}=27$ GeV. The nomenclatures of the smooth curves are as in Fig. 1.

with the counting rule corrected by the QCD Q^2 evolution. The results presented here are summed over the distinct subprocesses, e.g., the initial states for the fusion model are taken as gg and $q\bar{q}$ with $q=u$, d, s and for the cluster model as q_1q_2 with $q_{1,2}=u$ and d.

We take the QCD coupling constant as $\alpha(Q^2)$

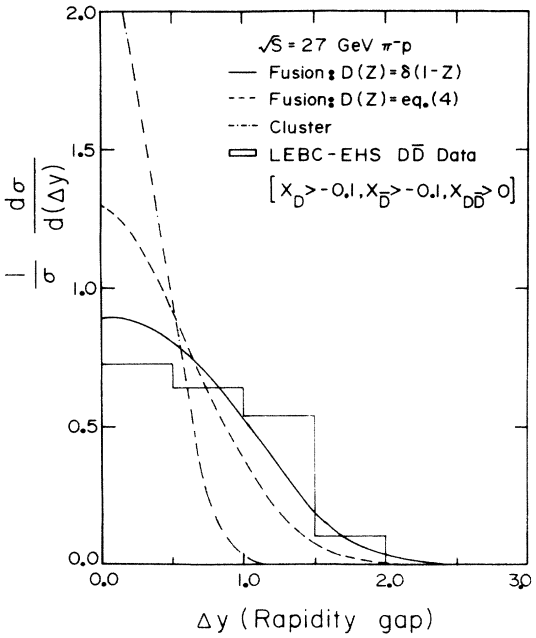

FIG. 4. Normalized distribution $(1/\sigma)d\sigma/d\Delta y$ as a function of the rapidity gap Δy between D and $\bar{D}$ at $\sqrt{s}=27$ GeV. The solid and the dashed curves are fusion-model calculations with $D(z)=\delta(1-z)$ and $D(z)=$Eq. (4), respectively. The dash-dotted curve refers to the cluster model. The histogram refers to the LEBC-EHS experiment (Ref. 19).

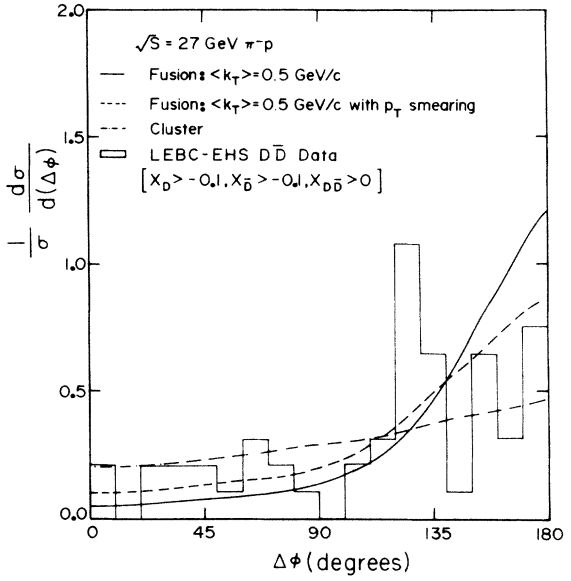

FIG. 5. Normalized distribution $(1/\sigma)d\sigma/d\Delta\phi$ as a function of azimuthal correlation angle $\Delta\phi$ between D and $\bar{D}$ at $\sqrt{s}=27$ GeV. The solid and the dashed curves are fusion-model calculation without and with p_T smearing at fragmentation. The dash-dotted curve refers to the cluster model with cluster mass of 5 GeV. The histogram refers to the LEBC-EHS experiment (Ref. 19).

$=12\pi/[25\ln(Q^2/\Lambda^2)]$ with Λ as 0.3 GeV. The mass of the charm quark and charm D meson are taken as 1.5 and 1.869 GeV, respectively. In the cluster model the nominal value of the cluster mass and the temperature parameter are taken as 5 GeV and 5 GeV^{-1}, respectively.

For the transverse-momentum distribution $f(k_T)$ of the

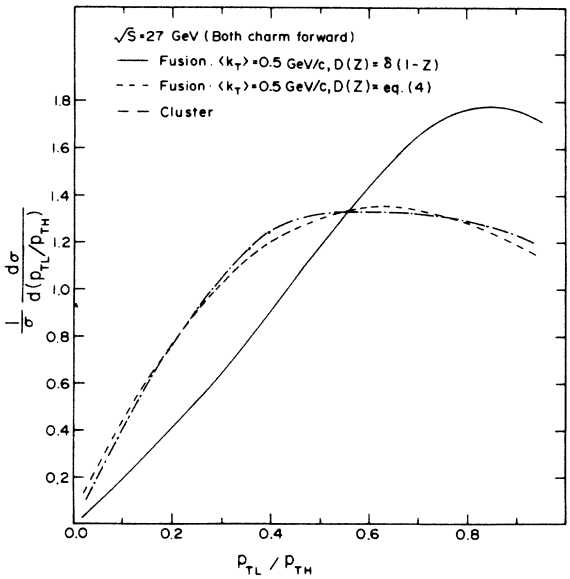

FIG. 6. Normalized distribution $(1/\sigma)d\sigma/d(p_{TL}/p_{TH})$ as a function of the ratio p_{TL}/p_{TH} of the two transverse momenta of the D and $\bar{D}$ with $p_{TL}\leq p_{TH}$ and D, $\bar{D}$ in the forward hemisphere at $\sqrt{s}=27$ GeV. The nomenclatures of the smooth curves are as in Fig. 4.

TABLE I. Fusion model: Mean values of the distributions with $\langle k_T \rangle = 0.5$ GeV/c, $\hat{s}_{\rm th} = 4m_c^2$, and $m_c = 1.5$ GeV.

$\sqrt{s}$ (GeV)	Fragmentation function	$\langle x \rangle$	$\langle p_T^2 \rangle$ [(GeV/c)^2]	$\langle M_{D\bar{D}} \rangle$ (GeV/c^2)	$\langle \Delta y \rangle$	$\langle \Delta\phi \rangle$ (degrees)	$\langle p_{TL}/p_{TH} \rangle$
27 ($\pi^- p$)	None	0.12	1.23	4.67	0.81	137.6	0.63
27 ($\pi^- p$)	$\delta(1-z)$	0.11	1.23	4.69	0.70	137.6	0.63
27 ($\pi^- p$)	Eq. (4)	0.06	0.55	4.10	0.50	137.6	0.56
27 (pp)	None	0.10	1.23	4.62	0.82	137.4	0.63
27 (pp)	$\delta(1-z)$	0.10	1.23	4.66	0.72	137.4	0.63
27 (pp)	Eq. (4)	0.06	0.55	4.08	0.50	137.4	0.56
62 (pp)	None	0.08	1.50	5.15	1.03	143.8	0.65
62 (pp)	$\delta(1-z)$	0.07	1.50	5.17	0.91	143.8	0.65
62 (pp)	Eq. (4)	0.04	0.71	4.31	0.68	143.8	0.56

partons, needed for Eq. (5), we have used the Gaussian distribution $f(k_T) = (A/\pi)\exp(-Ak_T^2)$ with $A = \pi/(4\langle k_T \rangle^2)$. We have used various values of $\langle k_T \rangle$ to study its effects.

The numerical calculations using Eqs. (1) and (8) need multidimensional integrations. In order to check the final accuracy of the results we have used two independent methods to generate plots: (a) by performing direct integration of the expressions, and (b) by generating events by the Monte Carlo technique. The results obtained from the two methods are in good agreement.

The results of our calculation normalized to unit area are displayed in Figs. 1–6 and the mean values of the distributions are summarized in Tables I–VI. In these distributions x stands for the Feynman x variable, Δy for the rapidity gap, $M_{D\bar{D}}$ the effective mass, $\Delta\phi$ the difference of the two azimuthal angles, and p_{TL},p_{TH} are the two transverse momenta of D and $\bar{D}$ with $p_{TL} < p_{TH}$. Figures 3–6 refer to $\sqrt{s} = 27$ GeV with both the charm mesons having $x > -0.1$ and the $D\bar{D}$ pair with $x > 0$; this is to facilitate comparison with the current LEBC-EHS experiment.[17–19] Similarly, Tables III and IV refer to the mean values of the distributions when both the charm mesons are emitted in the forward hemisphere ($x > 0.0$) with the average transverse momentum of the colliding partons as 0.5 GeV/c.

A. Fusion model

(i) It is seen from Tables I and III that the distributions in $M_{D\bar{D}}$ and Δy become narrow by demanding both the charm particles in the forward hemisphere; the other distributions, e.g., x, p_T^2, $\Delta\phi$, and p_{TL}/p_{TH} are not affected by this restriction.

(ii) There is no significant difference in the distributions for $\pi^- p$ and pp at $\sqrt{s} = 27$ GeV.

(iii) The fraction of $D\bar{D}$ produced both in the forward hemisphere is 0.30 at $\sqrt{s} = 27$ GeV; this fraction is nearly energy independent.

(iv) The incorporation of the fragmentation function $D(z)$ of Eq. (4) gives in general a softer distribution compared to $D(z) = \delta(1-z)$. $\Delta\phi$ in Table I is independent of the fragmentation function because we have neglected the transverse-momentum smearing in the fragmentation. The effect of the transverse-momentum smearing is shown in Fig. 5 by the dashed curve for $\langle q_T \rangle = 0.25$ GeV, where q_T is the transverse momentum of the charm D with respect to the direction of the charm quark; it decreases the value of $\langle \Delta\phi \rangle$ by 10°.

(v) We have checked that the transverse momentum k_T of the colliding partons does not change the distributions in x, $M_{D\bar{D}}$, and Δy. However the distributions in p_T^2, $\Delta\phi$, and p_{TL}/p_{TH} are dependent on the choice of $\langle k_T \rangle$. All these distributions become flatter with the increase in $\langle k_T \rangle$, see Table V.

(vi) Experimental data of x and p_T^2 distributions are compared with the model predictions in Figs. 1 and 2. Both the distributions are better reproduced with the fragmentation function $D(z) = \delta(1-z)$ compared to $D(z)$ with Eq. (4). It may be mentioned that the experimental values with $x > 0.5$ are larger than the prediction [see Fig. 1(a)].

(vii) $D\bar{D}$ correlation data shown in Figs. 3 and 5 are reasonably reproduced by the fragmentation function $D(z) = \delta(1-z)$; on the other hand, the fragmentation function of Eq. (4) gives softer distributions in $M_{D\bar{D}}$ and Δy and they are not in agreement with the data. The average values of $M_{D\bar{D}}$ and Δy for $D(z) = \delta(1-z)$ are 4.6 GeV/c^2 and 0.66, while for $D(z)$ with Eq. (4) they are 4.1 GeV/c^2 and 0.50; these values are to be compared with experimental values of $\langle M_{D\bar{D}} \rangle = 4.50 \pm 0.16$ GeV/c^2 and $\langle \Delta y \rangle = 0.80 \pm 0.14$ (Ref. 19).

TABLE II. Cluster model: Mean values of the distributions with cluster mass as 5 GeV.

$\sqrt{s}$ (GeV)	$\langle x \rangle$	$\langle p_T^2 \rangle$ [(GeV/c)^2]	$\langle M_{D\bar{D}} \rangle$ (GeV/c^2)	$\langle \Delta y \rangle$	$\langle \Delta\phi \rangle$ (degrees)	$\langle p_{TL}/p_{TH} \rangle$
27 ($\pi^- p$)	0.12	0.75	3.94	0.28	105.0	0.55
27 (pp)	0.10	0.74	3.94	0.28	104.7	0.55
62 (pp)	0.08	0.78	3.94	0.28	102.3	0.55

TABLE III. Fusion model: Mean values of the distributions with ($\langle k_T \rangle = 0.5$ GeV/c) when both the charm particles are emitted in the forward hemisphere (i.e., with $x_{D,\bar{D}} > 0$).

$\sqrt{s}$ (GeV)	Fragmentation function	$\langle M_{D\bar{D}} \rangle$ (GeV/c^2)	$\langle \Delta y \rangle$	$\langle \Delta\phi \rangle$ (degrees)	$\langle p_{TL}/p_{TH} \rangle$
27 ($\pi^- p$)	$\delta(1-z)$	4.46	0.50	138.0	0.63
27 ($\pi^- p$)	Eq. (4)	4.04	0.39	138.0	0.55
27 (pp)	$\delta(1-z)$	4.40	0.47	137.0	0.63
27 (pp)	Eq. (4)	4.0	0.35	137.0	0.55

B. Cluster model

(i) The distributions are not changed significantly by demanding both the charm particles in the forward hemisphere.

(ii) There is also no significant difference in the distributions for $\pi^- p$ and pp at $\sqrt{s} = 27$ GeV.

(iii) The fraction of $D\bar{D}$ produced both in the forward hemisphere is 0.45, i.e., the majority of the charm pairs are produced in the same hemisphere.

(iv) The transverse momentum of the colliding partons does not play any significant role in this model as the $D\bar{D}$ are the decay products of the cluster and hence are not directly related to the colliding partons unlike in the fusion model.

(v) The crucial parameters in this model are the mass of the cluster M and the temperature k. The mean values of the various distributions at $\sqrt{s} = 27$ GeV are summarized in Table VI for three different values of the cluster mass and in Table VII for three different values of the temperature. The noticeable change is in the $p_T{}^2$ distribution, which becomes broader with the increase in the cluster mass and narrower with the increase in the temperature. [It may be mentioned that the $p_T{}^2$ distribution as obtained via the double inclusive distribution of Eq. (8) is a little bit narrower compared to that obtained via the single inclusive distribution.[26] It arises because of an extra input of independent emission of $D\bar{D}$ from the fragmentation of the cluster in Eq. (8). This does not affect the x distribution.] The other distributions are not changed significantly for variations in M and k in the range $5 < M < 7$ GeV and $3 < k < 7$ GeV^{-1}.

(vi) Experimental data of x and $p_T{}^2$ distributions are reasonably reproduced by the model; however, it may be mentioned that the experimental values with $x > 0.5$ are larger than the prediction, see Fig. 1(a).

(vii) $D\bar{D}$ correlation data as shown in Figs. 3–5 are not reproduced by the model. The rapidity gap (Δy) as well as the $M_{D\bar{D}}$ distribution are much narrower compared to the data. The distribution in $\Delta\phi$ is somewhat flatter than the experimental distribution which basically reflects the hypothesis of independent emission of $D\bar{D}$ from the cluster.

We have also considered two alternative emission schemes of $D\bar{D}$ from the cluster. These are (a) D and $\bar{D}$ emitted back to back in the cluster rest frame, and (b) emission as in (a) with a further constraint of D and $\bar{D}$ having equal momentum in the cluster rest frame. These schemes are intended to maximize the broadening of the Δy and the $M_{D\bar{D}}$ distributions. The mean values of the distributions in Δy, $M_{D\bar{D}}$, $\Delta\phi$, and p_{TL}/p_{TH} are summarized in Table VIII. As expected the $\Delta\phi$ distribution (not shown) has a sharp peak at 180° for both the schemes (a) and (b) and this results in $\langle \Delta\phi \rangle \approx 140°$. This is in disagreement with the experimental observation[19] of $115 \pm 8°$. There is broadening in the Δy and the $M_{D\bar{D}}$ distribution in the schemes (a) and (b); however, the effect is not sufficient to reproduce the experimental data—the experimental values are $\langle \Delta y \rangle = 0.80 \pm 0.14$ and $\langle M_{D\bar{D}} \rangle = 4.5 \pm 0.16$ GeV/c^2 (Ref. 19).

C. Comparison of the two models

(i) x distributions in the fusion model with $D(z) = \delta(1-z)$ and in the cluster model are nearly the same.

(ii) $p_T{}^2$ distribution in the cluster model falls rapidly beyond $p_T > 1.5$ GeV/c, compared to the fusion model, because of the restriction in cluster mass to 5 GeV.

(iii) $M_{D\bar{D}}$ and the rapidity-gap distributions are both much narrower in the cluster model compared to the predictions of the fusion model.

(iv) $\Delta\phi$ distribution is much flatter in the cluster model

TABLE IV. Cluster model: Mean values of the distributions when both the charm particles are emitted in the forward hemisphere (i.e., with $x_{D,\bar{D}} > 0$) and cluster mass as 5 GeV.

$\sqrt{s}$ (GeV)	$\langle M_{D\bar{D}} \rangle$ (GeV/c^2)	$\langle \Delta y \rangle$	$\langle \Delta\phi \rangle$ (degrees)	$\langle p_{TL}/p_{TH} \rangle$
27 ($\pi^- p$)	3.92	0.27	104.9	0.55
27 (pp)	3.91	0.26	104.9	0.55

TABLE V. Fusion model: Mean values of the distributions at $\sqrt{s} = 27$ GeV for different values of $\langle k_T \rangle$ of the colliding partons.

Parton $\langle k_T \rangle$ (GeV/c)	Fragmentation function	$\langle p_T{}^2 \rangle$ [(GeV/c)^2]	$\langle \Delta\phi \rangle$ (degrees)	$\langle p_{TL}/p_{TH} \rangle$
0.1	$\delta(1-z)$	1.03	170.5	0.83
	Eq. (4)	0.44	170.5	0.65
0.5	$\delta(1-z)$	1.23	137.4	0.63
	Eq. (4)	0.55	137.4	0.56
0.9	$\delta(1-z)$	1.48	116.0	0.56
	Eq. (4)	0.66	116.0	0.50

TABLE VI. Cluster model: Mean values of the distributions at $\sqrt{s}=27$ GeV ($\pi^- p$) for different values of the cluster mass (temperature $k=5$ GeV^{-1}).

Cluster mass (GeV)	$\langle x\rangle$	$\langle p_T{}^2\rangle$ [(GeV/c)^2]	$\langle M_{D\bar{D}}\rangle$ (GeV/c^2)	$\langle \Delta y\rangle$	$\langle \Delta\phi\rangle$ (degrees)	$\langle p_{TL}/p_{TH}\rangle$
5	0.12	0.75	3.94	0.28	105.0	0.55
6	0.11	0.86	4.0	0.30	97.0	0.54
7	0.10	0.87	4.03	0.31	92.0	0.54

compared to the fusion-model prediction with $\langle k_T\rangle=0.5$ GeV.

(v) The ratio of the transverse momentum of the two D's (p_{TL}/p_{TH}) in the fusion model with $D(z)$ as Eq. (4) is similar to that in the cluster model.

(vi) The cluster model predicts more charm pairs in the same hemisphere compared to the fusion model.

IV. SUMMARY

In this paper we have made a detailed study of the $D\bar{D}$ correlations in the framework of fusion and cluster models which have both central-type production characteristics for charm particles in hadronic collisions. In the fusion model we have incorporated two forms for the fragmentation function: (i) $D(z)=\delta(1-z)$ and (ii) $D(z)$ as given by Eq. (4) which describes the D production in e^+e^- experiments; x and $p_T{}^2$ distribution of the charm production at $\sqrt{s}=27$ and 62 GeV are better reproduced by the form (i). The cluster model also reproduces the experimental distributions of x and $p_T{}^2$.

The major differences in the two models are in their predictions of the rapidity-gap and $M_{D\bar{D}}$ distributions. Both these distributions are much narrower in the cluster model compared to the fusion model. In the fusion model the fragmentation function of form (i) gives a broader distribution compared to form (ii). By restricting both the $D\bar{D}$ in the forward hemisphere the rapidity-gap distribution becomes narrower in the fusion model, whereas the cluster-model prediction remains unchanged.

The azimuthal-correlation ($\Delta\phi$) distribution is strongly dependent on $\langle k_T\rangle$ of the colliding partons in the fusion model, whereas in the cluster model it is independent of the k_T and the distribution is much flatter.

We have compared these two models with the available experimental data on $D\bar{D}$ correlation at $\sqrt{s}=27$ GeV. The experimental data are reasonably reproduced by the fusion model with the fragmentation function of form (i). On the other hand, the cluster model is not able to reproduce the correlation data.

APPENDIX A: DOUBLE INCLUSIVE DISTRIBUTION IN THE FUSION MODEL

In the c.m. frame of the hadron A and hadron B collision we define four-momentum vectors for the subprocess $a+b\to 1+2$, with $1\to 3$ and $2\to 4$ as used in the text, Sec. II A, where 1 and 2 are the charm quarks (c and $\bar{c}$) and 3 and 4 are the final charm hadrons (D and $\bar{D}$), as

$$\begin{aligned}
P_a&=(E_a=\hat{m}_a\cosh y_a,k_{Tax},k_{Tay},x_a\sqrt{s}/2=\hat{m}_a\sinh y_a)\ ,\\
P_b&=(E_b=\hat{m}_b\cosh y_b,k_{Tbx},k_{Tby},-x_b\sqrt{s}/2=\hat{m}_b\sinh y_b)\ ,\\
P_1&=(E_1=\hat{m}_1\cosh y_1,p_{T1},0,\hat{m}_1\sinh y_1)\ ,\\
P_2&=(E_2=\hat{m}_2\cosh y_2,p_{T2x},p_{T2y},\hat{m}_2\sinh y_2)\ ,\\
P_3&=(E_3=\hat{m}_3\cosh y_3,p_{T3},0,\hat{m}_3\sinh y_3)\ ,\\
P_4&=(E_4=\hat{m}_4\cosh y_4,p_{T4x},p_{T4y},\hat{m}_4\sinh y_4)\ .
\end{aligned}\tag{A1}$$

The colliding partons a and b are treated as massless. We have taken the incident hadron A along the positive z axis and the x axis has been defined along the transverse-momentum vector of the charm hadron 3; $x_{a,b}$ are the longitudinal momentum fractions and $\mathbf{k}_{Ta,b}$ are the effective transverse momenta of the colliding partons a,b in the incident hadrons A,B, respectively. $\hat{m}_i$ is the transverse mass, e.g., $\hat{m}_3{}^2=p_{T3}{}^2+M^2$ with M as the mass of 3. The invariant cross section for the subprocess $a+b\to 1+2$ at a fixed value of the square of the subprocesses energy, $\hat{s}=(P_a+P_b)^2$, can be written as

$$\begin{aligned}
d\sigma=&(\hat{s}/2\pi)(d\hat{\sigma}/d\hat{t})(d^3p_1/E_1)(d^3p_2/E_2)\\
&\times\delta^4(P_a+P_b-P_1-P_2)\ ,
\end{aligned}\tag{A2}$$

where $\hat{t}$ is the square of the four-momentum transfer between the parton a and the charm quark 1. The fragmentations of $1\to 3$ and $2\to 4$ are implemented through variables $z_3=|\mathbf{p}_3|/|\mathbf{p}_1|$ and $z_4=|\mathbf{p}_4|/|\mathbf{p}_2|$ with their distributions as $D(z_3)$ and $D(z_4)$; the momenta of 3 and 4 are taken to be collinear to 1 and 2, respectively. Now

TABLE VII. Cluster model: Mean values of the distributions at $\sqrt{s}=27$ GeV ($\pi^- p$) for different values of the temperature parameter k (cluster mass fixed at 5 GeV).

k (GeV^{-1})	$\langle x\rangle$	$\langle p_T{}^2\rangle$ [(GeV/c)^2]	$\langle M_{D\bar{D}}\rangle$ (GeV/c^2)	$\langle \Delta y\rangle$	$\langle \Delta\phi\rangle$ (degrees)	$\langle p_{TL}/p_{TH}\rangle$
3.0	0.12	0.92	3.98	0.32	110.2	0.55
5.0	0.12	0.75	3.94	0.28	105.0	0.55
7.0	0.11	0.62	3.90	0.26	97.3	0.55

TABLE VIII. Cluster model: Mean values of the distributions at $\sqrt{s}=27$ GeV for three different emission schemes of $D\bar{D}$ (cluster mass=5 GeV and temperature $k=5$ GeV^{-1}).

Emission scheme	$M_{D\bar{D}}$ (GeV/c^2)	$\langle \Delta y \rangle$	$\langle \Delta\phi \rangle$ (degrees)	$\langle p_{TL}/p_{TH} \rangle$
Independent emission	3.94	0.28	105.0	0.55
Scheme (a)[a]	4.16	0.43	141.0	0.60
Scheme (b)[a]	4.22	0.44	141.8	0.65

[a]See text for details.

changing the volume elements $d^3p_{1,2}$ to $d^3p_{3,4}$ and folding in the parton's probability distributions in the colliding hadrons, we obtain the following expression for the double inclusive cross section for the charm hadrons:

$$E_3E_4\frac{d\sigma}{d^3p_3d^3p_4}=\int\frac{\hat{s}}{2\pi}\frac{d\hat{\sigma}}{d\hat{t}}\frac{E_3E_4}{E_1E_2}\frac{D(z_3)}{z_3^3}\frac{D(z_4)}{z_4^3}G_{a/A}(x_a,\mathbf{k}_{Ta},Q^2)\times G_{b/B}(x_b,\mathbf{k}_{Tb},Q^2)dz_3dz_4dx_adx_bd^2\mathbf{k}_{Ta}d^2\mathbf{k}_{Tb}\times\delta^4(P_a+P_b-P_1-P_2)\,, \tag{A3}$$

where the function $G_{i/H}$ describes the probability distribution of the parton i inside the hadron H; see Eq. (5) for its relation to the structure function $F_{i/H}$. We now integrate out x_a, x_b, and $\mathbf{k}_{Ta}$ using the four δ functions:

$$E_3E_4\frac{d\sigma}{d^3p_3d^3p_4}=\int\frac{\hat{s}}{2\pi}\frac{d\hat{\sigma}}{d\hat{t}}\frac{E_3E_4}{E_1E_2}\frac{D(z_3)}{z_3^3}\frac{D(z_4)}{z_4^3}JG_{a/A}(x_a,\mathbf{k}_{Ta},Q^2)\times G_{b/B}(x_b,\mathbf{k}_{Tb},Q^2)dz_3dz_4d^2\mathbf{k}_{Tb} \tag{A4}$$

with

$$J=(4/s)\,|\cosh y_a\cosh y_b/\sinh(y_a-y_b)|\,.$$

$y_{a,b}(y_a>0,y_b<0)$ and $\mathbf{k}_{Ta}$ are determined by solving the four conservation equations. They are given by

$$\sinh y_b=(-AB\pm\sqrt{C}\,)/D\,,$$
$$\sinh y_a=(A-k_{Tb}\sinh y_b)/k_{Ta}\,,$$
$$k_{Ta}^2=(p_{T1}+p_{T2x}-k_{Tbx})^2+(p_{T2y}-k_{Tby})^2\,,$$

where

$$A=\hat{m}_1\sinh y_1+\hat{m}_2\sinh y_2\,,$$
$$B=k_{Ta}^2-k_{Tb}^2-E^2+A^2\,,\quad E=E_1+E_2\,,$$
$$C=E^2(B^2+4A^2k_{Tb}^2-4E^2k_{Tb}^2)\,,$$
$$D=2k_{Tb}(E^2-A^2)\,.$$

APPENDIX B: DOUBLE INCLUSIVE DISTRIBUTION IN THE CLUSTER MODEL

For the production and decay of a cluster via the subprocess $a+b\to1+2$ and $1\to3+4+X$, where 1 is the cluster, we define the four-momentum vectors in the c.m. frame of the colliding hadrons A and B as

$$\begin{aligned}&P_a=(x_a\sqrt{s}\,/2,0,0,x_a\sqrt{s}\,/2)\,,\\&P_b=(x_b\sqrt{s}\,/2,0,0,-x_b\sqrt{s}\,/2)\,,\\&P_1=(E_1=\hat{M}\cosh y_1,p_{T1x},p_{T1y}\,,\ p_{z1}=\hat{M}\sinh y_1)\,,\\&P_3=(E_3,p_{T3},0,p_{z3})\,,\\&P_4=(E_4,p_{T4x},p_{T4y},p_{z4})\,.\end{aligned} \tag{B1}$$

Quarks a, b, and 2 are treated as massless and M is the mass of the cluster 1. The positive z axis is taken along the direction of a; the colliding quarks are assumed to have no transverse momentum.

The double inclusive distribution for the charm hadrons 3 and 4 can be written as

$$E_3E_4\frac{d\sigma}{d^3p_3d^3p_4}=\int D_C(1\to3+4+x)E_1\frac{d\sigma}{d^3p_1}\frac{d^3p_1}{E_1} \tag{B2}$$

with D_C as the fragmentation function of the cluster, see Eq. (9) of the text. The production distribution of the cluster can be written by folding parton's probability distributions in Eq. (A2) as

$$E_1\frac{d\sigma}{d^3p_1}=\int\frac{\hat{s}}{2\pi}\frac{d\sigma}{d\hat{t}}\frac{1}{E_2}\frac{F(x_a)F(x_b)}{x_ax_b}\times dx_adx_b\delta(E_a+E_b-E_1-E_2)\,, \tag{B3}$$

where $\hat{t}=M^2-x_a\sqrt{s}\,(E_1-p_{z1})$ and $E_2^2=(\mathbf{p}_a+\mathbf{p}_b-\mathbf{p}_1)^2$. Substituting (B3) in Eq. (B2) and integrating out dy_1 of d^3p_1/E_1 with the help of the δ function we get

$$E_3E_4\frac{d\sigma}{d^3p_3d^3p_4}=\int\frac{\hat{s}}{\pi}\frac{1}{|Z|}D_C\frac{d\sigma}{d\hat{t}}\frac{F(x_a)F(x_b)}{x_ax_b}\times dx_adx_bd^2\mathbf{p}_{T1}\,, \tag{B4}$$

where

$$Z=\hat{M}\sqrt{s}\,[(x_a-x_b)\cosh y_1-(x_a+x_b)\sinh y_1]\,.$$

Energy conservation yields the following relation for y_1:

$$\sinh y_1=[\sqrt{s}\,(x_a-x_b)(\hat{s}+M^2)\pm\sqrt{A}\,]/(4\hat{s}\hat{M}) \tag{B5}$$

with

$$A=(\hat{s}+M^2)^2[s(x_a-x_b)^2+4\hat{s}]-4s\hat{s}\hat{M}^2(x_a+x_b)^2\,.$$

[1]CERN-Dortmund-Heidelberg-Saclay (CDHS) Collaboration, T. Hansl *et al.*, Phys. Lett. **74B**, 139 (1978).
[2]CDHS Collaboration, H. Abramowicz *et al.*, Z. Phys. C **13**, 179 (1982).
[3]Big European Bubble Chamber (BEBC) Collaboration, P. Fritze *et al.*, Phys. Lett. **96B**, 427 (1980).
[4]CERN-Hamburg-Amsterdam-Rome-Moscow (CHARM) Collaboration, M. Jonker *et al.*, Phys. Lett. **96B**, 435 (1980).
[5]R. C. Ball *et al.*, Phys. Rev. Lett. **51**, 143 (1983).
[6]J. L. Ritchie *et al.*, Phys. Lett. **126B**, 499 (1983).
[7]M. Basile *et al.*, Lett. Nuovo Cimento **33**, 17 (1981).
[8]M. Basile *et al.*, Lett. Nuovo Cimento **33**, 33 (1981).
[9]LEBC-EHS Collaboration, M. Aguilar-Benitez *et al.*, Phys. Lett. **123B**, 98 (1983).
[10]LEBC-EHS Collaboration, M. Aguilar-Benitez *et al.*, Phys. Lett. **123B**, 103 (1983).
[11]LEBC-EHS Collaboration, M. Aguilar-Benitez *et al.*, Phys. Lett. **135B**, 237 (1984).
[12]T. Aziz *et al.*, Nucl. Phys. **B199**, 424 (1982); Z. Phys. C **26**, 13 (1984); **27**, 325 (1985).
[13]T. Aziz and A. Gurtu, Z. Phys. C **21**, 137 (1983).
[14]W. Geist and S. Reucroft, CERN Yellow Report No. 83-02, 1983, Vol. II, p. 190.
[15]S. Reucroft, in *Multiparticle Dynamics, 1983,* proceedings of the XIV International Symposium, Lake Tahoe, edited by J. F. Gunion and P. M. Yager (World Scientific, Singapore, 1983); and also Report No. CERN/EP 83-155, 1983 (unpublished).
[16]D. P. Roy, in *New Particle Production,* proceedings of the XIX Rencontre de Moriond, edited by J. Tran Thanh Van (Editions Frontiéres, France, 1984); and also Report No. DO-TH 84/09, 1984 (unpublished).
[17]LEBC-EHS Collaboration, M. Aguilar-Benitez *et al.*, Phys. Lett. **146B**, 266 (1984).
[18]LEBC-EHS Collaboration, M. Aguilar-Benitez *et al.*, Phys. Lett. **161B**, 400 (1985).
[19]LEBC-EHS Collaboration, M. Aguilar-Benitez *et al.*, Phys. Lett. **164B**, 404 (1985).
[20]B. L. Combridge, Nucl. Phys. **B151**, 427 (1979).
[21]C. E. Carlson and R. Suaya, Phys. Lett. **81B**, 329 (1979).
[22]R. Winder and C. Michael, Nucl. Phys. **B173**, 59 (1980).
[23]V. Barger *et al.*, Phys. Rev. D **25**, 112 (1982).
[24]R. Odorico, Nucl. Phys. **B209**, 77 (1982).
[25]R. M. Godbole and D. P. Roy, Phys. Rev. Lett. **48**, 1711 (1982).
[26]D. P. Roy and B. R. Desai, Z. Phys. C **22**, 149 (1984).
[27]S. N. Ganguli and M. Shouten, Z. Phys. C **19**, 83 (1983).
[28]S. N. Ganguli, Z. Phys. C **21**, 163 (1983).
[29]B. Andersson *et al.*, Lund Report No. LUTP 83-4, 1983 (unpublished).
[30]C. Peterson *et al.*, Phys. Rev. D **27**, 105 (1983).
[31]R. P. Feynman *et al.*, Nucl. Phys. **B128**, 1 (1977).
[32]M. Suzuki, Phys. Lett. **71B**, 139 (1977).
[33]A. J. Buras and K. J. F. Gaemers, Nucl. Phys. **B132**, 249 (1978).
[34]J. F. Owens and E. Reya, Phys. Rev. D **17**, 3003 (1978).
[35]CDHS Collaboration, H. Abramowicz *et al.*, Z. Phys. C **12**, 289 (1982).